NANOSCALE COMPOSITIONAL ANALYSIS OF AN ANTARCTIC MICROMETEORITE USING ATOM PROBE TOMOGRAPHY. M. R. Boyd[1], J. A. Cartwright[1], J. Singh[2], P. A. J. Bagot[2] & M. P. Moody[2], [1]Department of Geological Sciences, University of Alabama, Box 870338, Tuscaloosa, AL 35487, USA; [2]Department of Materials, University of Oxford, 16 Parks Road, Oxford, OX1 3PH, UK. E-mail: mrboyd4@crimson.ua.edu

Introduction: The term 'cosmic dust' describes micrometre-sized extra-terrestrial material. Micrometeorites (MMs) represent a collection of this material, 10 µm to 2 mm in size [1], recovered from the Earth's surface. These particles undergo significant processesing in their journey to Earth, including atmospheric entry heating. MMs can be classified into three groups based on the degree of heating experienced: 1) 'unmelted' MMs that have undergone no melting; 2) 'scoriacious' MMs that have been partially melted; and 3) 'cosmic spherules', which are fully melted particles [2]. Of these groups, cosmic spherules offer prime candidates for the analysis of textures and compositions related to frictional heating with the atmosphere.

The degree of heating that a cosmic dust particle experiences is connected to its flight path, namely the velocity and incidence angle, as well as its initial size [3,4]. These parameters may be related to the particle's source. For example, simulated entry velocities for comet-derived dust particles are >12 km/s, compared to ~5 km/s for asteroidal particles [5]. This difference will have an effect on the intensity and duration of heating [6], which in turn, will have some control on the resulting compositional and textural features observed in ablated MMs.

Investigating MM composition and texture, and comparing these characteristics to previous analytical evidence and models of MM atmospheric entry, may shed light on the changes caused by atmospheric processing. For example, zinc (Zn) and sulphur (S) depletions have been identified in stratospheric particles [7]; the loss of these volatile elements may place constraints on the temperatures experienced by MMs during heating [8]. A nanometre-scale investigation of MMs would further determine mineral or elemental trends that could be used as a proxy for entry heating.

Recently, atom probe tomography (APT) has been demonstrated as a powerful tool for characterization of extra-terrestrial processing in lunar dust grains [9], a compositional boundary in an iron meteorite [10], and nano-crystalline features within a chondrule [11,12]. Here, we investigate two regions of interest (ROIs) within a cosmic dust particle that target a compositional boundary. With APT, we obtain 3D spatial and compositional maps with nanometre-scale resolution.

Samples & Method: A cosmic spherule, CS94_03, was selected from a collection of MMs recovered from blue ice near Cap Prud'homme, Antarctica, in 1994 by Maurette et al. [13,14]. Preliminary analyses performed at the Alabama Analytical Research Center (AARC), University of Alabama (UA), using an electron probe microanalyser (EPMA), revealed distinct rim and core regions in back-scattered electron (BSE) images (Fig.1) and compositional layering demonstrated by energy-dispersive spectroscopy (EDS), notably in iron (Fe), oxygen (O), and to a lesser extent, silicon (Si) [14].

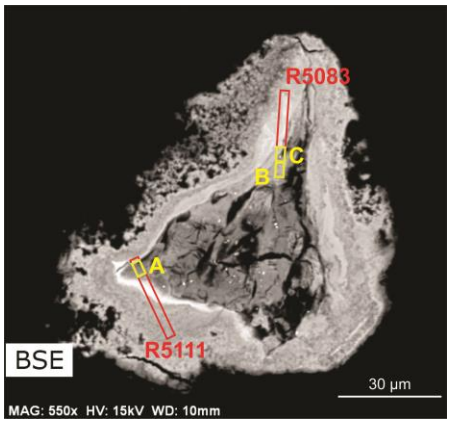

Figure 1: BSE image of MM CS94_03, showing the ROIs targeted for lift-out (red) and the successful APT tips (yellow).

Site-specific sample preparation was performed using a ZEISS Crossbeam 540 and a ZEISS NVision 40, equipped with a gallium (Ga) focused ion beam (FIB) at the University of Oxford (UO), to create lamellae R5111 and R5083, respectively (Figs.1, 2.a). These lamellae were selected to intersect the core-rim boundary and to sample the compositional layering evident in BSE and EDS images (Fig.1). APT needles were created from R5111 and R5083 (Fig.2.b) and run on a LEAP-5000XS and LEAP-5000XR, respectively, at UO. Results were obtained for needle A from lamella R5111 in two stages (i.e., A1, the 'top' tip, and A2, the 'bottom' tip), and for needles B and C from the R5083 lamella. The output HITS data files were processed using Cameca's IVAS software at the AARC.

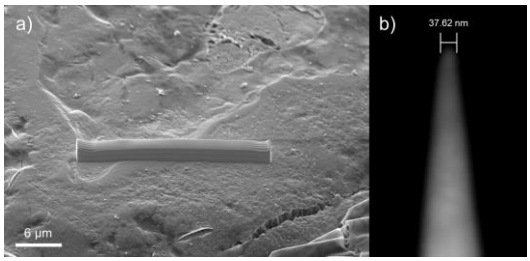

Figure 2: Site-specific sample preparation: a) platinum (Pt) bar with ~2 µm thickness placed over the R5111 ROI; b) APT needle 'A' milled from the lamella prepared in (a).

Results & Discussion: We identify nanometre-scale lineations in tip A1 from the R5111 lamella, predominantly in metallic elements and their associated complex ions: Fe and FeO (Fig.3.a), Zn, aluminium (Al), copper (Cu), titanium oxide (TiO), manganese (Mn) and manganese oxide (MnO). The lineations for these species overlap with one another and extend throughout the tip with a ~3-5 nm width. In this tip, we also find a cluster of chromium (Cr) and its associated complex oxide ions: CrO_2 (Fig.3.b) and CrO_3. The lineations pervade into the bottom tip, A2, of this needle, though not as sharply. However, SiO shows distinct concentrations with the same orientation as the metallic lineations. Additionally, Zn, Mn and Fe are heterogeneously distributed to one side of the tip.

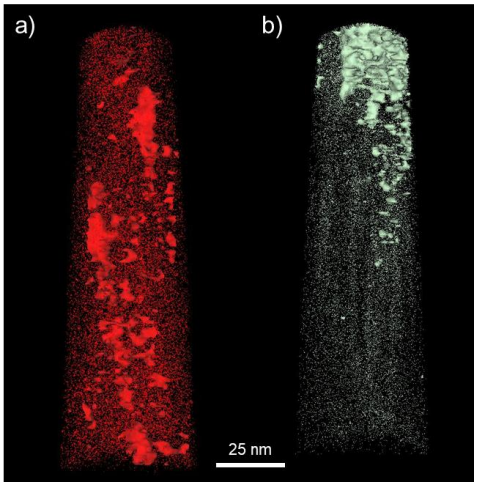

Figure 3: Tip A1 reconstruction from the R5111 lamella: a) FeO lineations, including a 40% atomic concentration isosurface (ACI); b) CrO_2 cluster, including a 2.5% ACI.

The linear features and partitioning of Zn, Mn and Fe in needle A suggest a relationship between the behaviour of top row transition metals, and may result from elemental diffusion during atmospheric entry heating. It is possible that the Cr-rich region represents a chromite spinel grain; similar features have previously been identified as relict phases in MMs [16] and in previous APT analysis of a chondrule [11,12]. However, this interpretation is tentative, given that surface oxidation can occur during sample transport and storage [17].

Tip B shows a sharp compositional boundary (Fig.4), with carbon (C), magnesium (Mg), hydrogen (H), O, SiO_2, Ti, and Cr concentrated in the lower half, whilst the top half is primarily composed of FeO, FeO_2 and some Zn. This boundary indicates elemental partitioning, and shows an FeO enrichment. Such an enrichment may have formed by oxidation of Fe during atmospheric entry, similar to the magnetite coatings that form on meteorites during atmospheric entry [18].

Concluding Remarks: These APT results, which we believe to be the first obtained for cosmic dust, demonstrate the success of performing nanometre-scale analyses on such materials. Furthermore, the results reveal the presence of nanometre-scale features and heterogeneities within the MM that are not visible at lower resolutions.

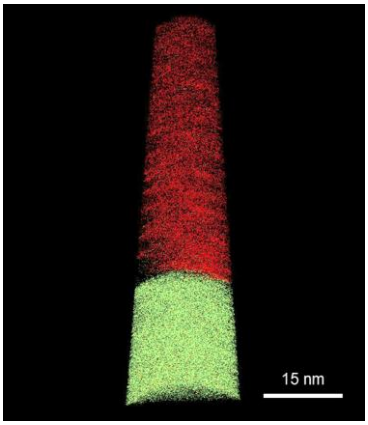

Figure 4: APT reconstruction for tip 'B' from R5083, showing carbon (green), FeO (red), and the compositional boundary.

The consequences of atmospheric entry heating are dependent on several factors, including particle velocity, duration of heating and precursor composition. We will compare these results to micro- and nanoscale analyses of other cosmic dust particles to identify differences in the extent of atmospheric processing, with the aim of determining the parameters that exert a control over these processes.

Acknowledgements: We are grateful to M. Genge (Imperial College London) for providing us with the collection of Antarctic MMs. The authors also thank R. Holler and S. Deb at the AARC (UA).

References: [1] Rubin A.E. and Grossman J.N. (2010) *Meteorit. Planet. Sci., 45*, 114-122. [2] Genge M.J. et al. (2008) *Meteorit. Planet. Sci., 43*, 497-515. [3] Genge M.J. (2017) *Geophys. Res. Lett.*, 44, 1679-1686. [4] Carrillo-Sánchez J.D. et al. (2015) *Geophys. Res. Lett.*, 42, 6518-6525. [5] Zook H.A. and Jackson A.A. (1992) *Icarus*, 97, 70-84. [6] Toppani A. et al. (2001) *Meteorit. Planet. Sci.*, 36, 1377-1396. [7] Flynn G.J. and Sutton S.R. (1992) *Proc. Lunar Planet. Sci.*, 22, 171-184. [8] Greshake A. et al. (1998) *Meteorit. Planet. Sci.*, 33, 267-290. [9] Greer J. et al. (2020) *Meteorit. Planet. Sci.*, 55, 426-440. [10] Rout S.S. et al. (2017) *Meteorit. Planet. Sci.*, 52, 2707-2729. [11] Cartwright J.A. et al. (2017) *AGU 2017*, #P51A-2558. [12] Cartwright J.A. et al. (2018) *Goldschmidt 2018*, 346. [13] Maurette M. et al. (1991) *Nature, 351*, 44-47. [14] Maurette M. et al. (1992) *Meteoritics, 27*, 257. [15] Boyd M.R. and Cartwright J.A. (2020) *LPSC 51*, #2799. [16] Taylor S. et al. (2012) *Meteorit. Planet. Sci.*, 47, 550-564. [17] Herbig M. et al. (2020) *Microsc. Res. Tech.*, 1-7. [18] Genge M.J. et al. (1997) *Geochim. Cosmochim. Acta*, 61, 5149-5162.